The Uncertainty Principle in Classical Optics

MASUD MANSURIPUR

In the classical electromagnetic theory the wave-vector $\boldsymbol{k} = (2\pi/\lambda)\sigma$ underlies the Fourier space of propagating (or radiative) fields. The $\boldsymbol{k}$-vector combines into a single entity the wavelength λ and the unit vector σ that signifies the beam's propagation direction. The Fourier transform relation between the three-dimensional space of everyday experience and the space of the wave-vectors (the so-called $\boldsymbol{k}$-space) gives rise to relationships between the two domains analogous to Heisenberg's uncertainty relations.

Considering that in quantum theory the electromagnetic $\boldsymbol{k}$-vector is proportional to the photon's momentum[1] ($\boldsymbol{p} = \hbar\boldsymbol{k}$, where $\hbar = h/2\pi$, h being the Planck constant), one should not be surprised to find relationships between dimensions of a beam in the XYZ-space and its momentum spread in the $\boldsymbol{k}$-space. Such relationships impose fundamental limits on the ability of measurement systems to determine the various properties of electromagnetic fields.

In this article we address two problems that have widespread applications in optical metrology, spectroscopy, telecommunications, etc., and discuss the constraints imposed by the uncertainty principle on these problems. The first topic of discussion is the separation of two overlapping beams of identical wavelength having slightly different propagation directions. This will be followed by an analysis of the limits of separating co-propagating beams having slightly different wavelengths.

Angular separation and the limit of resolvability

Figure 1 shows an aperture of diameter D, which transmits two plane waves of the same wavelength λ propagating in slightly different directions. Denoting the angular separation between the beams by $\Delta\theta$, we find that the projections of the two $\boldsymbol{k}$-vectors along the X-axis differ by $\Delta k_x \approx (2\pi/\lambda)\Delta\theta$. In geometrical optics, rays propagate along straight lines and, therefore, the two beams must separate from each other after a certain propagation distance. In wave optics, however, the beams expand as they propagate along Z and, although their centers drift apart, there is the distinct possibility that they will never be completely separated. Roughly speaking, we expect the beams to remain more or less collimated between $z = 0$ and $z = D^2/\lambda$, the Rayleigh range[2] for a beam of diameter D and wavelength λ. If at the Rayleigh range the distance between the beam centers is greater than D, the beams should be separable; otherwise their drifting apart will go hand in hand with their expansion, and the beams remain entangled as they propagate beyond the Rayleigh range. The necessary condition for separability is thus $(D^2/\lambda)\Delta\theta > D$, or equivalently,

$$D\Delta k_x > 2\pi. \qquad (1)$$

The lower bound 2π on the product of D and Δk_x appearing in Ineq. (1) is not exact, but depends on the definition of beam diameter D and the adopted criterion for separability, which are typically imprecise. For all practical purposes, the number appearing on the right-hand side of Ineq. (1) should be on the order of unity, say, greater than 1 but less than 10.

Invoking the quantum nature of light, if the aperture diameter D is interpreted as a measure of the uncertainty Δx about the photon position along X, while Δk_x is related (through the relation $\boldsymbol{p} = \hbar\boldsymbol{k}$) to the linear momentum uncertainty Δp_x along the same axis, then Ineq. (1) is equivalent to Heisenberg's uncertainty relation $\Delta x\,\Delta p_x > h$.

Figure 2 shows the intensity and phase profiles of two plane waves as well as those of their superposition at the aperture depicted in Fig. 1 (diameter $D = 500\lambda$). The phase distributions in Figs. 2(b) and 2(d) indicate that one of the beams is slightly tilted towards the upper right corner of the XY-plane, while the other is tilted by an equal amount towards the lower left corner. The angular separation between these beams is $\Delta\theta = 0.23° = 0.004$ radians. The combined beam's intensity distribution in Fig. 2(e) reveals the angular separation of the two superimposed beams through a tell-tale fringe pattern.

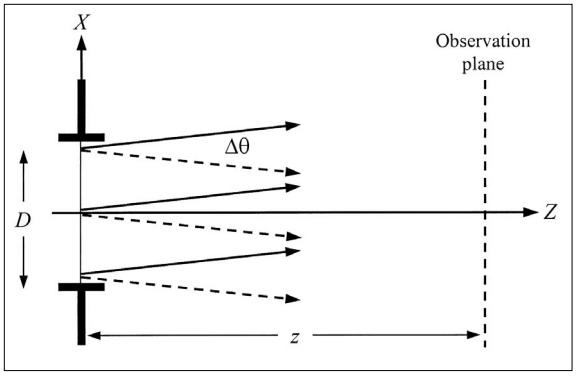

Figure 1. Two beams of the same wavelength λ, propagating in slightly different directions, pass through an aperture of diameter D. The angle between the two $\boldsymbol{k}$-vectors is $\Delta\theta$, giving rise to $\Delta k_x \approx (2\pi/\lambda)\Delta\theta$. The beams separate from each other at the observation plane located a distance z from the aperture, provided the uncertainty relation $D\Delta k_x \geq 2\pi$ is satisfied.

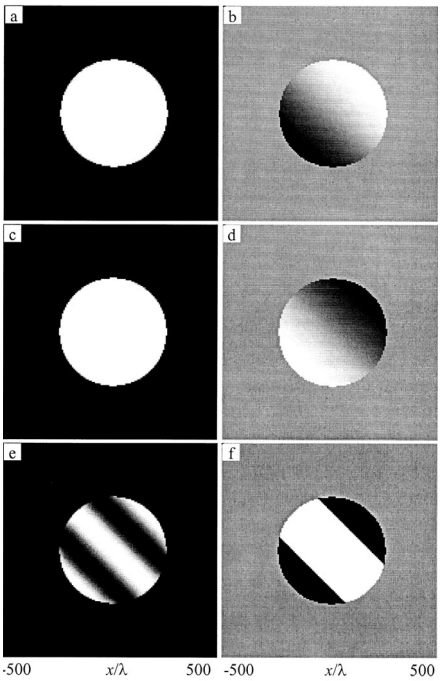

Figure 2. Plots of intensity (left) and phase (right) at the entrance aperture of the system of Fig. 1. Two uniform beams, one propagating with a slight tilt toward the upper right, another with a slight tilt toward the lower left, enter a $D = 500\lambda$ aperture. The angular separation of the beams is $\Delta\theta = 0.23°$. The individual beams are shown in the top (a, b) and the middle (c, d) rows; their superposition appears at the bottom (e, f).

When the composite beam (whose intensity and phase distributions are shown in Figs. 2(e, f)) is propagated along the *Z*-axis, one obtains at various distances from the aperture the intensity patterns displayed in Fig. 3.[3] It is seen in these pictures that the two constituent beams continue to overlap at first, giving rise to interesting interference patterns. After a sufficient propagation distance, however, the beams separate and go their own ways. The assumed value of $D\,\Delta k_x$ in this example is 4π, which satisfies Ineq. (1).

Separating two beams by means of a lens

In the preceding section it was demonstrated that separating two beams of a certain angular distance $\Delta\theta$ requires a minimum beam diameter D in accordance with Ineq. (1). It may be asked whether a similar limitation exists on the propagation distance z before the individual beams can be resolved. Apparently no physical law limits the required distance z, although practical considerations seem to impose certain constraints. In free space, the required propagation distance is typically less than or equal to the Rayleigh range, D^2/λ, but one can substantially reduce this distance by employing a lens, as shown in Fig. 4. Here two overlapping beams of diameter D and angular separation $\Delta\theta$ are resolved after going through an aberration-free lens. In the focal plane of the lens the center-to-center spacing of the focused spots is $f\,\Delta\theta$, which must be greater than the Airy disk[4] radius of $\sim 0.6\lambda/\mathrm{NA} = 1.2\,f\lambda/D$. Note that the resolvability criterion is independent of f and NA, requiring only that $D\,(\Delta\theta/\lambda) > 1.2$, which is a statement of the uncertainty principle in the present context. The required propagation distance f in this example can be much less than that needed in the case of free-space propagation of Fig. 1. It must be emphasized that the uncertainty principle does not impose any constraints on z, the requirement for resolvability being only a restriction on the product of D and $\Delta\theta$.

An interesting feature of separating two beams by means of a lens is the resulting dependence of the focused spots on the state of polarization. To reduce the required propagation distance z, one may use a high-NA lens, thus enhancing the polarization effects. The shortest focal length f is obtained when the NA of the lens is close to unity, that is, $f \approx \frac{1}{2}D$. Figure 5 shows computed plots of intensity distribution at the focal plane of an NA = 0.99, $f = 250\lambda$ lens, when the incident beam is the two-beam superposition depicted in Fig. 2.[3] The three columns of Fig. 5 represent three different polarization states. In (a) both incident beams are linearly polarized along *X*, which explains the elongation of the spots in this particular direction. In (b) the two beams are linearly polarized at 45° to the *X*- and *Y*-axes, i.e., the direction along which the spots are separated from each other. The plot in (c) corresponds to the case when both beams are circularly polarized. Frames (d)-(f) are the logarithmic versions of those in (a)-(c), showing their detailed structure by emphasizing the weaker regions. Since the assumed values of $D = 500\lambda$ and $\Delta\theta = 0.004$ rad satisfy the uncertainty relation in Ineq. (1), the focused spots are seen to be resolved irrespective of their polarization state.

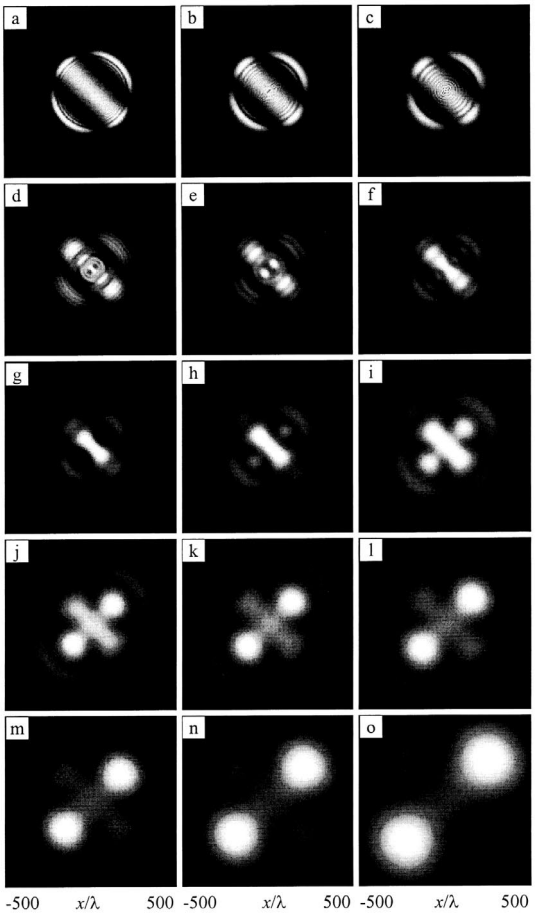

Figure 3. Two overlapping plane waves depicted in Fig. 2 propagate along the *Z*-axis. The various intensity patterns in frames (a) to (o) are obtained at $z/(10^3\lambda)$ = 1, 2, 3, 10, 20, 30, 40, 50, 60, 70, 80, 90, 100, 125, and 150, respectively. Initially the beams strongly interfere with each other, but as propagation proceeds, they separate and exhibit their individual identities.

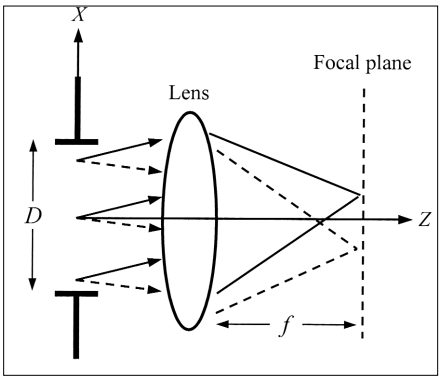

Figure 4. Two identical beams of diameter D and angular separation $\Delta\theta$ may be isolated after going through an aberration-free lens. In the focal plane, the distance between the focused spots is $f\,\Delta\theta$, which must be greater than the Airy disk radius of $1.2f\lambda/D$ if the individual spots are to be resolved.

Angular discrimination by means of a Fabry-Pérot etalon

Another device that can, in principle, accomplish the separation of two beams via angular discrimination is a Fabry-Pérot etalon,[4,5] such as that shown in Fig. 6. This particular etalon is tuned to transmit a plane wave of $\lambda = 633$ nm at the incidence angle of $\theta = 45°$. Figure 7 shows the etalon's computed reflection and transmission coefficients, $r_s = |r_s|\exp(i\phi_{rs})$ and $t_s = |t_s|\exp(i\phi_{ts})$, versus θ for an s-polarized plane-wave of $\lambda = 633$ nm. It turns out that the shapes of the transfer functions $|r_s(\theta)|$ and $|t_s(\theta)|$ are not quite suitable for complete separation of two finite-diameter beams of differing propagation directions.

Computed plots of intensity distribution in Fig. 8 confirm that the etalon of Fig. 6 can only partially separate two beams of diameter $D = 2 \times 10^4\lambda$ and angular separation $\Delta\theta = 0.115° = 0.002$ rad, even though the value of $D\,(\Delta\theta/\lambda) = 40$ in this case amply satisfies Ineq. (1). Figure 8(a) shows the incident pattern of intensity distribution of the superposed beams upon arriving at the etalon. One of these

beams propagates along the direction that makes a 45° angle with the etalon's surface normal, while the other deviates from this direction by $\Delta\theta = 0.115°$. The reflected intensity profile depicted in Fig. 8(b) contains mostly the latter beam, plus a small fraction of the former. This is due to the imperfect transfer function of the etalon, which cannot fully transmit the angular spectrum of the 45° beam, nor can it fully reflect the spectrum of the 45.115° beam. Either beam's angular spectrum has a width of $\sim\lambda/D \approx 0.003°$, which would readily pass through a narrow rectangular transfer function, but is partially blocked by the sharply peaked transfer functions of the etalon (see Fig. 7(a)). The same arguments apply to the transmitted intensity distribution shown in Fig. 8(c) which, although primarily composed of the 45° incident beam, still contains a fraction of the 45.115° beam.[3]

To summarize the results of this and the preceding sections, there are several ways of separating two overlapping beams of the same wavelength and differing propagation directions. Some of these methods may be more effective than others, but none could violate the uncertainty relation given by Ineq. (1). Moreover, Ineq. (1) remains valid even if the beams are observed within a transparent medium of refractive index $n > 1$. For instance, in Fig. 1 if the region to the right of the aperture happens to be filled with such a medium, the angular separation $\Delta\theta$ of the beams shrinks by a factor n upon entering the medium, but the length of the $\boldsymbol{k}$-vector increases by the same factor, thus preserving the magnitude of Δk_x. Similarly, in Fig. 4 if the index of the medium on the right-hand-side of the lens happens to be n, the focused spot diameters will be n times smaller, but their center-to-center spacing will also be reduced by the same factor, resulting once again in the preservation of Ineq. (1).

Co-propagating beams of differing wavelengths

A problem of general interest in spectroscopy is that of separating two beams of slightly different wavelengths, λ_1 and λ_2, propagating in the same direction. In this case the beam diameter D turns out to be irrelevant, but the available propagation distance z is critical for isolating the individual beams.

A straightforward method of separating two beams of differing wavelengths is shown in Fig. 9. This Mach-Zehnder interferometer[4] splits each input beam into two equal halves, provides a separate path for each half, then recombines the halves into a single beam at the output. For one of the wavelengths, say, λ_1, the path-length difference Δz between the two arms of the device may be an integer-multiple of λ_1, in which case the corresponding half-beams interfere constructively and emerge from one exit channel of the interferometer. For the other wavelength, λ_2, the path-length difference may be a half-integer-multiple of λ_2, in which case interference will be destructive and the beam will emerge from a different exit channel of the device. Therefore, separability condition for this interferometer is $\Delta z/\lambda_1 - \Delta z/\lambda_2 = \frac{1}{2}$, or

$$\Delta z\,\Delta k_z \approx 2\pi\,\Delta z\,\Delta\lambda/\lambda^2 = \pi. \qquad (2)$$

Figure 10 shows computed detector signals S_1, S_2 of the system of Fig. 9 versus the input wavelength in the vicinity of $\lambda = 633$ nm.[3] For the particular path-length difference chosen in this example ($\Delta z = 1.266$ mm), it is observed that, in compliance with Eq. (2), a pair of beams having $\Delta\lambda = 0.158$ nm can be readily separated from each other.

An alternative form of the uncertainty relation may be obtained in this case by invoking the quantum mechanical relation between the magnitude k of the wave-vector and the photon energy $E = h\nu$, namely, $k = 2\pi/\lambda = 2\pi\nu/c = E/\hbar c$. For two beams of wavelengths λ and $\lambda + \Delta\lambda$, co-propagating in the Z direction, $\Delta k_z = \Delta E/\hbar c$. Also $\Delta z = c\Delta t$, where c is the speed of light and Δt is the time needed for light to travel a distance Δz in free space. The product $\Delta z\,\Delta k_z$ is thus proportional to $\Delta E\,\Delta t$, with $\hbar$ being the proportionality constant. One may thus reinterpret Eq. (2) as a statement of the time-versus-energy uncertainty. When the observations are made in a transparent medium of refractive index $n > 1$, the increase of the $\boldsymbol{k}$-vector by a factor of n dictates a corresponding decrease in Δz. This

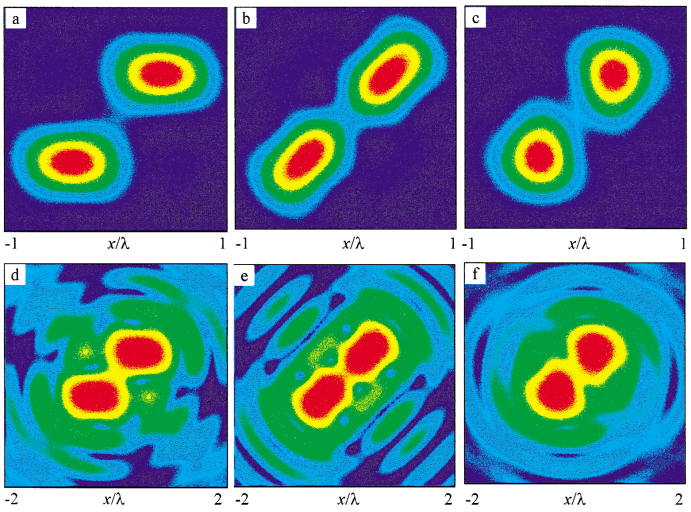

Figure 5. Total electric field intensity distribution ($|E|^2 = |E_x|^2 + |E_y|^2 + |E_z|^2$) at the focal plane of a 0.99NA lens. (Rainbow colors: red = maximum, blue = minimum). The beam at the entrance pupil is the superposition of two $D = 500\lambda$ beams of angular separation $\Delta\theta = 0.23°$, as shown in Fig. 2. In (a) the assumed polarization state of both incident beams is linear along the X-axis. In (b) the two beams are linearly polarized at 45° to the X-axis, i.e., along the direction of separation of the spots. In (c) one of the beams is right-circularly polarized, while the other is left-circularly polarized. Frames (d)-(f) in the bottom row are the logarithmic versions of frames (a)-(c) in the top row. Like an overexposed photographic plate, a logarithmic plot reveals weak regions of an intensity distribution.

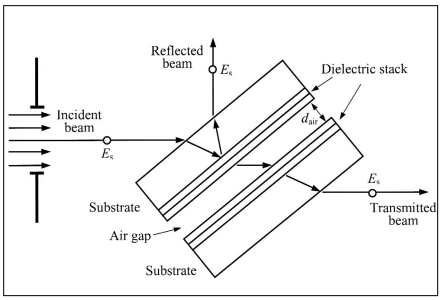

Figure 6. Fabry-Pérot etalon designed for operation at $\lambda = 633$ nm, $\theta = 45°$. Dielectric mirrors each contain six pairs of high/low-index layers ($n_1 = 2.0$, $d_1 = 84.6$ nm; $n_2 = 1.5$, $d_2 = 119.6$ nm). Both mirror substrates are glass ($n_{sub} = 1.5$), and the medium separating the mirrors is air ($d_{air} = 55.95$ μm). The incidence angle on the etalon is in the vicinity of $\theta = 45°$; within the substrate, however, the angle of incidence on the stack is close to $\theta' = 28.1255°$ ($\sin\theta = n_{sub}\sin\theta'$). The etalon can separate two beams of identical λ arriving through an aperture of diameter D, but differing in propagation direction, namely, $\theta_1 = 45°$, $\theta_2 = 45° + \Delta\theta$. One beam is reflected by the etalon while the other is transmitted. Only s-polarized light is considered here, although p-polarized beams exhibit similar behavior.

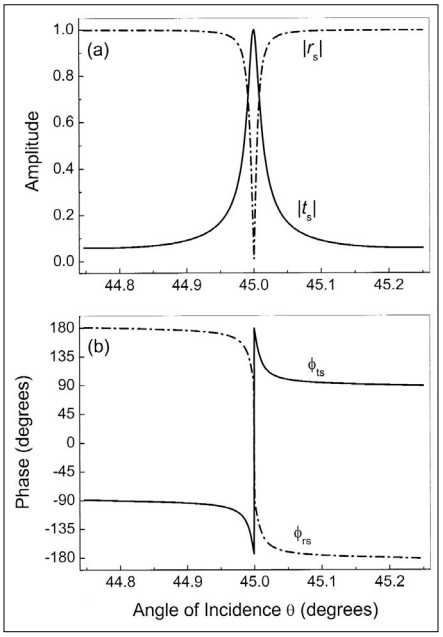

Figure 7. Computed reflection and transmission coefficients versus the incidence angle θ for the etalon of Fig. 6 at λ = 633 nm for an s-polarized plane wave. The magnitude and phase of the reflection and transmission coefficients are defined through the relations $r_s = |r_s| \exp(i\phi_{rs})$ and $t_s = |t_s| \exp(i\phi_{ts})$. At λ = 633 nm the stack is tuned to fully transmit at θ = 45°. A small deviation from 45° incidence causes a sharp drop in $|t_s|$ and a corresponding rise in $|r_s|$.

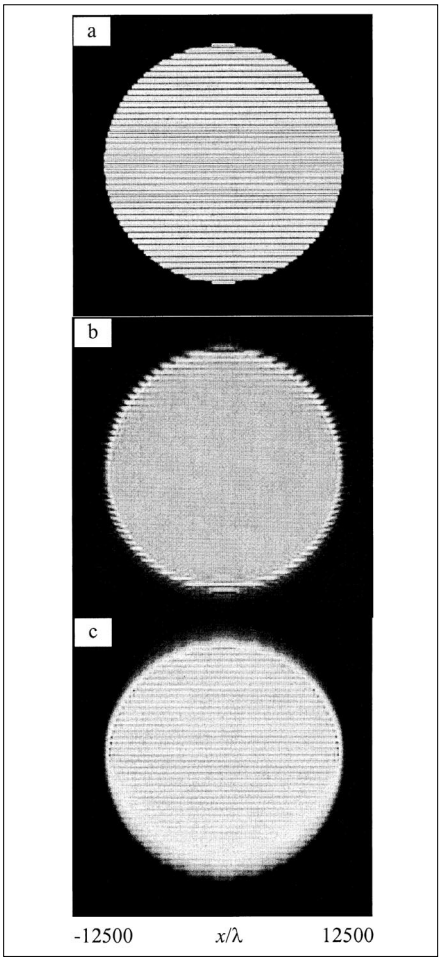

Figure 8. Two overlapping beams of uniform amplitude and circular cross-section (λ = 633 nm, $D = 2 \times 10^4\lambda$) arrive at the etalon of Fig. 6. One beam travels at θ = 45° relative to the etalon's surface normal, the other at θ = 45.115°. (a) Intensity distribution of the superposed beams at the entrance aperture. (b) Reflected intensity distribution, consisting mainly of the second beam plus a small fraction of the first. (c) Transmitted intensity distribution, consisting mostly of the first beam plus a small fraction of the second.

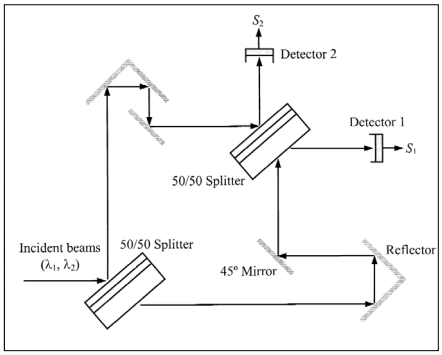

Figure 9. The Mach-Zehnder interferometer can be used to separate two beams of differing wavelengths, λ_1 and λ_2. The beams have identical diameters and arrive in the same direction. The two beams are split equally at the first 50/50 splitter, travel the two arms of the device, and are recombined at the second 50/50 splitter. The lengths of the two arms of the interferometer differ by Δz. When $\Delta z/\lambda_1 - \Delta z/\lambda_2 = \frac{1}{2}$, constructive interference at the second beam-splitter for one of the two wavelengths coincides with destructive interference for the other. The beams are thus separated at the second splitter, one is captured by detector 1, the other by detector 2. The 45° mirrors (three in each arm) have a reflectivity of 90%, resulting in an overall system transmission of 73%. The 50/50 splitters are identical, each consisting of a glass substrate coated with a six-layer dielectric stack as follows:

(Substrate, n_{sub} = 1.5) / (d_1 = 30 nm, n_1 = 2.64) / (d_2 = 140 nm, n_2 = 1.76) / (d_3 = 50 nm, n_3 = 2.64) / (d_4 = 105 nm, n_4 = 1.76) / (d_5 = 60 nm, n_5 = 2.64) / (d_6 = 100 nm, n_6 = 1.76) / Air

Although the above stack works for both p- and s-polarized light, its splitting ratio is much closer to 50/50 for s-light than for p-light. In our simulations the polarization state of the incident beam was fixed at s.

is consistent with the reduced speed of light in the medium of index n, which yields the same travel time Δt for the shorter propagation distance $\Delta z/n$. Needless to say, $\Delta E = h\Delta\nu$ is independent of n.

Wavelength discrimination using a Fabry-Pérot etalon

The etalon of Fig. 6 may also be used to separate co-propagating beams of slightly different wavelengths, say, λ and λ + Δλ. Figure 11 shows computed plots of reflection and transmission coefficients versus λ for a resonator having an air gap d_{air} = 55.95 μm. From Eq. (2) at λ = 633 nm, considering that $\Delta z = 2d_{air}\cos(45°)$ = 79.125 μm, we find Δλ = 2.53 nm, in agreement with the peak-to-valley distance in the simulated results of Fig. 11. The figure, however, indicates the feasibility of resolving beams with a smaller Δλ as well; this is due to the high finesse of the Fabry-Pérot etalon. In other words, multiple back and forth reflections within the etalon's cavity build up an optical field whose amplitude is G times stronger than that of the incident beam. (In the present example, G is 3.0 for s-light and 1.94 for p-light.) The effective Δz is thus G times the effective gap width, resulting in a corresponding increase in the resolution of the device.

Spectral analysis using a diffraction grating

Consider two co-propagating beams of wavelengths λ and λ + Δλ, where it is assumed for convenience that Δλ > 0. These beams travel along the Z-axis and pass through an aperture of diameter D. By definition, $k_z = 2\pi/\lambda$ and, therefore, $\Delta k_z = 2\pi\Delta\lambda/\lambda^2$. Figure 12 shows the above beams arriving at an incidence angle $0° \le \theta < 90°$ on a grating of period P. The N^{th} diffracted order emerges from the grating at an angle θ′, in accordance with Bragg's law,[4,5]

$$\sin\theta' = \sin\theta + N\lambda/P, \qquad (3a)$$

which yields,

$$\cos\theta'\,\Delta\theta' = (N/P)\Delta\lambda. \qquad (3b)$$

Now, the emergent beam diameter is $D' = D|\cos\theta'/\cos\theta|$. Since the lens is expected to resolve the two wavelengths, Ineq. (1) requires that $|\Delta\theta'| \ge \lambda/D'$, which leads to $|\cos\theta'\Delta\theta'| \ge \lambda\cos\theta/D$, which in turn leads

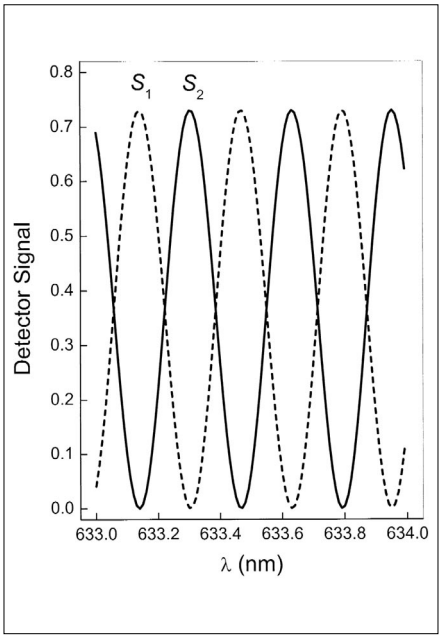

Figure 10. Computed detector signals S_1 and S_2 versus the input wavelength λ in the Mach-Zehnder interferometer of Fig. 9. The assumed path-length difference between the two arms of the device is Δz = 1.266 mm. In the vicinity of λ = 633 nm the adjacent peaks of S_1 and S_2 are separated by $\Delta\lambda$ = 0.158 nm, in agreement with Eq. (2).

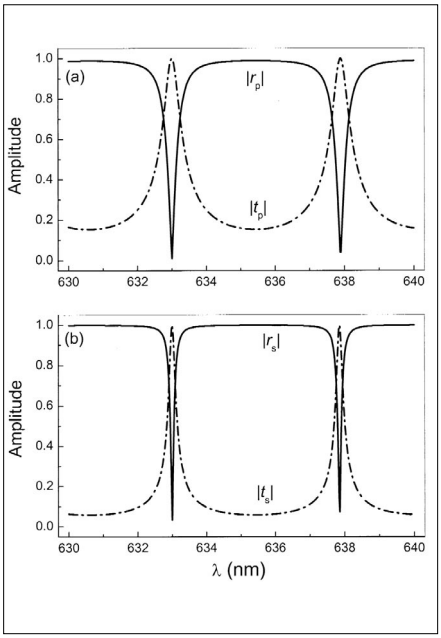

Figure 11. Computed plots of amplitude reflection and transmission coefficients versus λ for the Fabry-Pérot etalon depicted in Fig. 6. The air gap and the incidence angle are fixed at d_{air} = 55.95 μm and θ = 45°. The incident beam is p-polarized in (a) and s-polarized in (b).

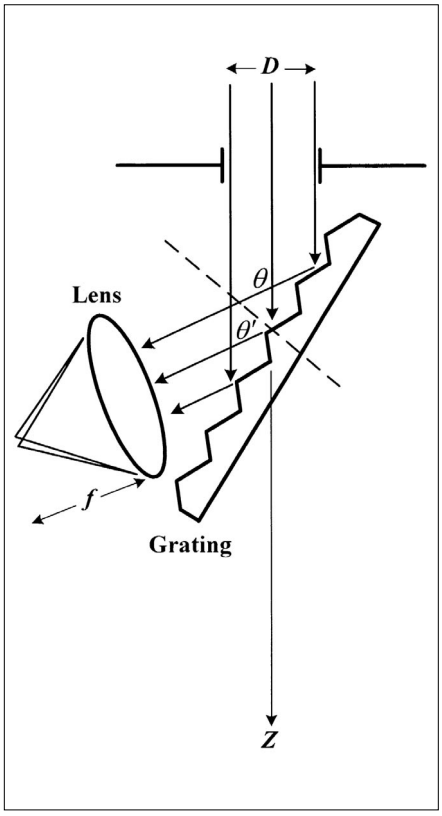

Figure 12. Two beams of wavelengths λ and λ+Δλ, propagating in the same direction *Z*, arrive at an aperture of diameter *D*. The beams propagate a distance Δz_1 from the center of the aperture to a grating of period *P*, shining on the grating at an angle θ. One of the diffracted orders (the N^{th} order) leaves the grating at an angle θ′, travels a distance Δz_2 (from the center of the grating to the center of the lens), then enters a lens of focal length *f* and numerical aperture NA ≈ 1. Emerging from the grating, the two wavelengths deviate from each other by an angle Δθ′, thus forming separate focused spots at the focal plane of the lens. From the entrance aperture to the focal plane, the total propagation distance is $\Delta z = \Delta z_1 + \Delta z_2 + f$.

to $|N/P|\,\Delta\lambda \geq \lambda\cos\theta/D$. In other words,

$$D/\cos\theta \geq (\lambda/\Delta\lambda)\,|P/N|. \qquad (4a)$$

From Eq. (3a) it is clear that $|N\lambda/P| \leq 2$, namely, $|P/N| \geq \frac{1}{2}\lambda$. Inequality (4a) may thus be written as follows:

$$D/\cos\theta \geq \tfrac{1}{2}\lambda^2/\Delta\lambda. \qquad (4b)$$

Inequality (4b) places a lower bound for resolvability not on the beam diameter *D*, but on the illuminated length of the grating, $D/\cos\theta$, in the direction perpendicular to the grooves.

Next we examine the propagation distance from the center of the entrance aperture to the focal plane of the lens. With reference to Fig. 12, the shortest possible distance from the entrance aperture to the grating center is $\Delta z_1 = \frac{1}{2}D\tan\theta$. Similarly, the shortest possible distance from the grating to the lens center (ignoring the possibility that the lens might block the incident beam) is $\Delta z_2 = \frac{1}{2}D'|\tan\theta'| = \frac{1}{2}D|\sin\theta'|/\cos\theta$. The smallest feasible focal length for the lens is $f = \frac{1}{2}D'$, corresponding to NA = 1. Therefore, the shortest distance Δz from the center of the entrance aperture to the focal plane of the lens is given by,

$$\Delta z = \Delta z_1 + \Delta z_2 + f \qquad (5a)$$
$$= \tfrac{1}{2}(D/\cos\theta)\,(\sin\theta + |\sin\theta'| + |\cos\theta'|).$$

Since $\sin\theta \geq 0$, and $|\sin\theta'| + |\cos\theta'| \geq 1$ for any θ′, Eq. (5a) yields,

$$\Delta z \geq \tfrac{1}{2}D/\cos\theta. \qquad (5b)$$

Combining Ineqs. (4b) and (5b) then yields $\Delta z \geq \frac{1}{4}\lambda^2/\Delta\lambda$, that is,

$$\Delta z\,\Delta k_z \geq \tfrac{1}{2}\pi. \qquad (6)$$

Note that the initial beam diameter *D* in this example is not restricted at all, whereas the propagation distance Δz is required to be greater than a certain minimum, $\frac{1}{4}\lambda^2/\Delta\lambda$, to ensure resolvability of the wavelengths λ and λ + Δλ.

Acknowledgment

I am grateful to Ewan M. Wright of the Optical Sciences Center for insightful suggestions.

References

1. R. P. Feynman, R. B. Leighton, and M. Sands, The Feynman Lectures on Physics, Addison-Wesley, Reading, Massachusetts (1964).
2. A. E. Siegman, Lasers, University Science Books, California (1986).
3. The simulations reported in this article were performed by DIFFRACT™, and MULTILAYER™; both programs are products of *MM Research, Inc.*, Tucson, Arizona.
4. M. Born and E. Wolf, Principles of Optics, 6th edition, Pergamon Press, Oxford, 1980.
5. M.V. Klein, Optics, Wiley, New York (1970).

OPN contributing editor Masud Mansuripur <masud @u.arizona.edu> is a professor of Optical Sciences at the University of Arizona in Tucson and president of *MM Research, Inc.*